# Enabling Heterogeneous Connectivity in Internet of Things: A Time-Reversal Approach

Yi Han[†‡], Yan Chen[⋆‡], Beibei Wang[†‡], and K. J. Ray Liu[†‡]
[†] Origin Wireless Inc., College Park, MD 20742, USA
[‡] ECE Dept., University of Maryland, College Park, MD 20742, USA
[⋆] School of EE, University of Electronic Science and Technology of China, Chengdu, Sichuan, China
Email: {yhan1990, yan, bebewang and kjrliu}@umd.edu

***Abstract*—With the pervasive presence of massive smart devices, Internet of Things (IoT) is enabled by wireless communication technology. The devices in IoT usually have very diverse bandwidth capabilities, and thus in need of many communication standards. To facilitate communications between these heterogeneous bandwidths of devices, middlewares have often been developed. However, they are often not suitable for resource-constrained scenario due to their complexity. It leads us to ask is there a unified approach that can support the communication between the devices with heterogeneous bandwidths? In this paper, we propose the time-reversal (TR) approach to answer such a question. A novel TR-based heterogeneous system is proposed, which can address the bandwidth heterogeneity and maintain the benefit of TR at the same time. Although there is an increase in complexity, it concentrates mostly on the digital processing of the access point (AP), which can be easily handled with more powerful digital signal processor (DSP). We further conduct the theoretical analysis of the interference in the proposed system. Simulations show the bit-error-rate (BER) performance can be significantly improved with appropriate spectrum allocation. Finally, Smart Homes is chosen as an example of IoT applications to evaluate the performance of the proposed system.**

***Index Terms*—Internet of things (IoT), bandwidth heterogeneity, Time-Reversal (TR)**

## I. Introduction

Ubiquitous RFID tags, sensors, actuators, mobile phones and etc. cut across many areas of modern-day living, which offers the ability to measure, infer and understand the environmental indicators. The proliferation of these devices creates the term of the Internet of Things (IoT), wherein these devices blend seamlessly with the environment around us, and the information is shared across the whole platform [1].

The notion of IoT dates back to the 1999, when it was first proposed by Ashton [2]. Even though logistic is the originally considered application, in the past decade, the coverage of IoT has been extended to a wide range of applications including healthcare, utilities, transport, etc. [3]. Thanks to the significant maturity and market size of wireless communication technologies such as ZigBee, Bluetooth, Wi-Fi, and near-field communication (NFC), IoT is on the path of transforming the current static Internet into a fully integrated future Internet [4]. Due to its high impact on several aspects of everyday life and behavior of the potential users [5], IoT is listed as one of six "Disruptive Civil Technologies" by the US National Intelligence Council with potential impacts on US national power [6].

Considering the massive amount of devices and various application scenarios in the IoT, the devices within the IoT are highly heterogeneous. From the perspective of communication, one of the significant heterogeneity is the bandwidth heterogeneity and thus the corresponding radio-frequency (RF) front-end. To address the bandwidth heterogeneity, various communication standards such as ZigBee, Bluetooth and Wi-Fi are adopted simultaneously in the current IoT platform, which leads to a wild growth of co-located wireless communication standards [7]. When multiple wireless communication standards are operated in the same geographical environment, the devices often suffer from harmful interference. Furthermore, the communication between devices with different communication standards is only possible through the use of gateway nodes, resulting in the fragmentation of the whole network, hampering the objects interoperability and slowing down the development of a unified reference model for IoT [8].

To enable the connectivity between devices with various bandwidths, some existing works build middlewares to hide the technical details of different communication standards from the application layer. In [9], Service Oriented Device Architecture (SODA) is proposed as a promising approach to integrate Service Oriented Architecture (SOA) principles into the IoT. An effective SOA-based integration of IoT is illustrated in enterprise service [10]. Business Process Execution Language (BPEL) has been widely used as the process language in the middleware [11]. However, these technologies used to realize middleware architectures are often not suitable for resource-constrained scenario due to their complexity.

Instead of building middlewares, is there any other more effective approach to enable the connectivity between the devices with different bandwidths? We try to answer this question by proposing the time-reversal (TR) approach. It is well known that radio signals will experience many multipaths due to the reflection from various scatters, especially in indoor environment. Through time-reversing (and conjugate, when complex-valued) the multipath profile as the beamforming signature, TR technique can constructively add up the signals of all the paths at the intended location, ending up with a spatio-temporal resonance effect [12]. As pointed out in [12], the TR technique is an ideal candidate for low-complexity, low

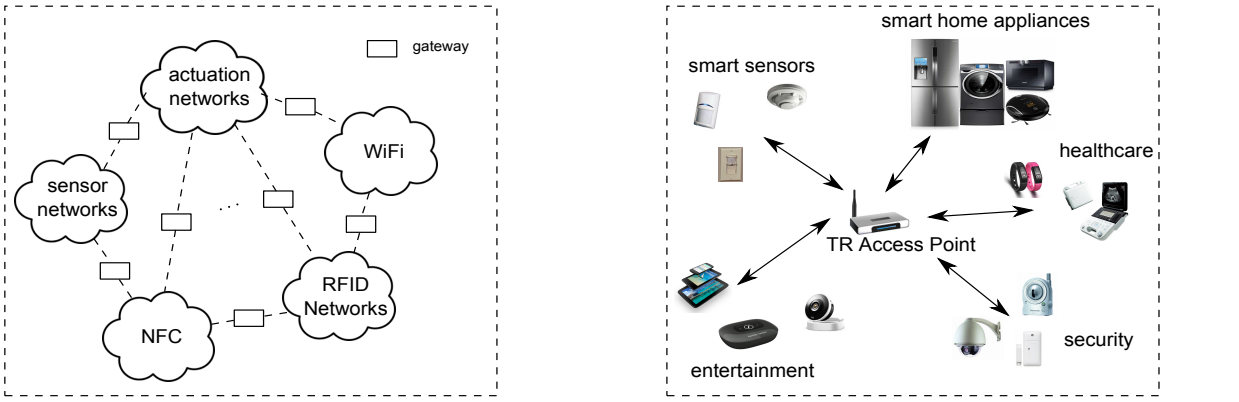


(a) An illustration of current IoT approach

(b) An illustration of heterogeneous TR-based IoT approach

Fig. 1: Comparison between existing IoT approach and heterogeneous TR-based IoT approach

energy consumption green wireless communication because of its inherent nature to fully harvest energy from all the paths. A TR-based multiuser media access scheme is proposed in [13], where only one-tap detection is needed at the device side resulting in low computational complexity and low cost of the terminal devices. With the unique location-specific signature, TR technique can provide additional physical-layer security and thus can enhance the privacy and security of customers in IoT. An overview of the TR wireless paradigm for green IoT has been presented in [14] summarizing all the promising features of TR technique. However, they cannot be directly applied to address the bandwidth heterogeneity in IoT, because of the implicit assumption that all terminal devices share the same bandwidth and thus the RF front-end.

In order to support devices with various bandwidths in IoT, a novel TR-based heterogeneous system is proposed in this paper, where a bank of various pulse-shaping filters are implemented to support data streams of different bandwidths. By integrating the multirate signal processing into TR technique, the proposed system is capable to support these heterogeneous devices with a single set of RF front-end, therefore it is a unified framework for connecting devices of heterogeneous bandwidths. As shown in Fig. 1, instead of connecting devices with different wireless communication standards through gateways and middlewares, the TR-based heterogeneous system in this paper directly links the devices together. The increase of complexity in the proposed system lies in the digital processing at the access point (AP), instead of at the devices' ends, which can be easily handled with more powerful digital signal processor (DSP). Meanwhile, the complexity of the terminal devices stays low and therefore satisfies the low-complexity and scalability requirement of IoT. Theoretical analysis of the interference is further conducted to predict the system performance. Simulation results show that the bit-error-rate (BER) performance can be significantly improved by the proposed TR-based heterogeneous system with appropriate spectrum allocation.

The rest of this paper is organized as follows. We first discuss the system architecture and working scheme of the existing homogeneous TR system in Section II. Based on the existing TR system, a TR-based heterogeneous system is developed in Section III. In Section IV, theoretical analysis regarding the interference in the proposed system is derived. Simulation results about the BER performance of the system are discussed in Section V. Finally, Section VI concludes the paper.

## II. Typical Homogeneous Time-Reversal System

In this section, we will first introduce the system architecture and working mechanism of the TR-based homogenous system, where the AP and all terminal devices (TDs) share the same spectrum thus the bandwidth and ADC sample rate.

A typical TR-based homogenous system is shown in Fig. 2 [14]. The channel impulse response (CIR) between the two transceivers is modeled as

$$h(t) = \sum_{v=1}^{V} h_v \delta(t - \tau_v) \tag{1}$$

where $h_v$ is the complex channel gain of $v^{th}$ path of the CIR, $\tau_v$ is the corresponding path delay, and $V$ is the total number of the independent multipaths in the environment (assuming infinite system bandwidth and time resolution). Without loss of generality, we assume that $\tau_1 = 0$ in the rest of paper, i.e., the first path arrives at time $t = 0$, and as a result, the delay spread of the multipath channel $\tau_C$ is given by $\tau_C = \tau_V - \tau_1 = \tau_V$.

Considering the practical communication system with limited bandwidth, pulse shaping filters are typically deployed to limit the effective bandwidth of transmission. In practice, raised-cosine filter is typically utilized as a pulse shaping filter which minimizes the inter-symbol-interference (ISI) [15]. Generally, the raised-cosine filter is splitted into two root-raised-cosine filters $\mathbf{RRC}_{B,f_s}[n]$ and deployed at each side of the transceivers, where $B$ is the available bandwidth and $f_s$ is the sample rate of the system. Based on the Nyquist rate [16], an $\alpha$-times oversampling (i.e. $f_s = \alpha B$) is practically implemented to counter the sampling frequency offset (SFO).

### A. Channel probing phase

As shown in Fig. 2(a), prior to AP's TR-transmission, an impulse is upsampled by $\alpha$, filtered by $\mathbf{RRC}_{B,f_s}[n]$ and transmitted out after going through the RF components at the

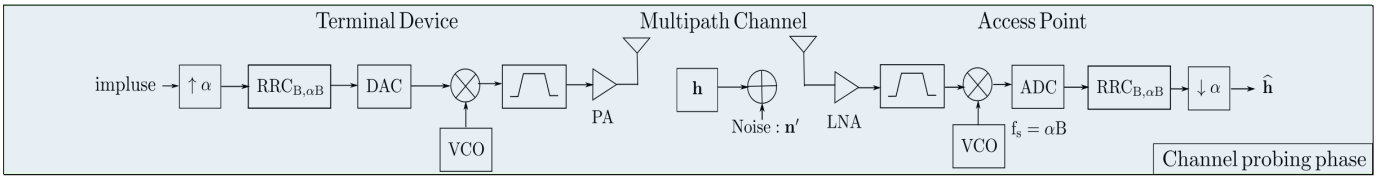


(a) Channel Probing Phase

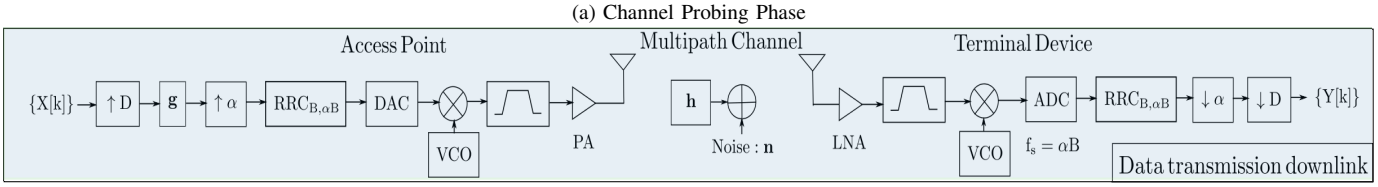


(b) Data Transmission Downlink

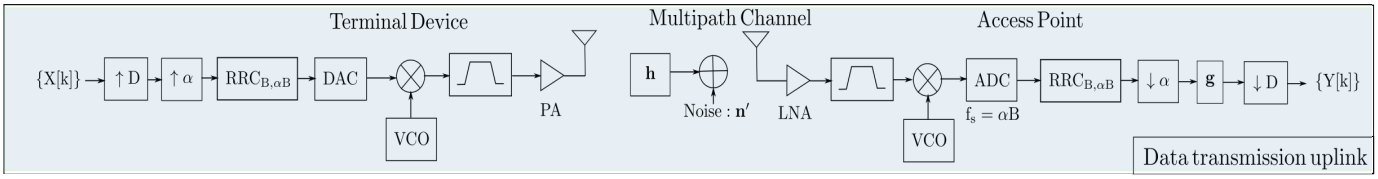


(c) Data Transmission Uplink

Fig. 2: Typical Homogeneous TR System

TD side. The transmitted signal propagates to AP through the multipath channel $h(t)$, where AP samples the received signal. Then the sampled signal goes through RF components, which later is filtered by another $\mathbf{RRC}_{B,f_s}[n]$, downsampled by $\alpha$, and finally recorded as the estimated CIR $\widehat{\mathbf{h}}$.

With sample rate $f_s = \alpha B$, the discrete CIR can be written as

$$\overline{h}[n] = \sum_{v=1}^{V} h_v \delta[nT_s - \tau_v] \tag{2}$$

where $T_s = 1/(\alpha B)$. Assume perfect channel estimation (noise and interference are ignored in the channel probing phase), the equivalent CIR between two RRC filters in Fig. 2(a) is written as

$$\widetilde{\mathbf{h}} = \left(\mathbf{RRC}_{B,f_s} * \overline{\mathbf{h}} * \mathbf{RRC}_{B,f_s}\right) \tag{3}$$

Based on the polyphase identity [17], the equivalent CIR (between the expander and decimator) for the system with bandwidth $B$ can be represented as

$$\widehat{\mathbf{h}} = \left(\mathbf{RRC}_{B,f_s} * \overline{\mathbf{h}} * \mathbf{RRC}_{B,f_s}\right)_{[\alpha]} \tag{4}$$

where $(\cdot)_{[\alpha]}$ represents $\alpha$-times decimation. From (4), one can see that those paths in (2), whose time differences are within the main lobe of raised-cosine filter, are mixed together for the system with a limited bandwidth $B$.

### *B. Data transmission phase*

Upon acquiring the equivalent CIR $\widehat{\mathbf{h}}$, different designs of signature waveforms (e.g. basic TR signature [12], ZF signature [18], and MMSE signature [19]) can be implemented at the AP side. With no loss of generality, the basic TR signature is considered in the rest of paper. In other words, the AP time-reverses (and conjugate, when complex-valued) the equivalent CIR $\widehat{\mathbf{h}}$, and uses the normalized TR waveform as the basic TR signature $\mathbf{g}$, i.e.,

$$g[n] = \frac{\widehat{h}^*[L-1-n]}{\|\widehat{\mathbf{h}}\|} \tag{5}$$

where $L$ is the number of taps in $\widehat{\mathbf{h}}$.

According to Fig. 2(b), there is a sequence of information symbols $\{X[k]\}$ to be transmitted to the TD. Typically, the symbol rate can be much lower than the system chip rate $(1/B)$. Therefore, a rate backoff factor $D$ is introduced to match the symbol rate with chip rate by inserting $(D-1)$ zeros between two symbols [12] [13] [20], i.e.,

$$X^{[D]}[k] = \begin{cases} X[k/D], & \text{if } (k \bmod D) = 0 \\ 0, & \text{if } (k \bmod D) \neq 0. \end{cases} \tag{6}$$

where $(\cdot)^{[D]}$ denotes the $D$-times interpolation. Consequently, the signature embedded symbols before the $\alpha$-times expander can be written as

$$S[k] = \left(\mathbf{X}^{[D]} * \mathbf{g}\right)[k]. \tag{7}$$

Based on the previous derivation in the channel probing phase, the system components between the expander and decimator in Fig. 2(b) can be replaced by $\widehat{\mathbf{h}}$. Therefore, the signal received at the TD side before the decimator with rate $D$ is the convolution of $S[k]$ and $\widehat{\mathbf{h}}$, plus additive white Gaussian noise (AWGN) $\widetilde{n}[k]$ with zero-mean and variance $\sigma_N^2$, i.e.,

$$Y^{[D]}[k] = \left(\mathbf{S} * \widehat{\mathbf{h}}\right)[k] + \widetilde{n}[k] \tag{8}$$

Then, TD decimates the symbols with backoff factor $D$ in

order to detect the information symbols $\{X[k]\}$, i.e.,

$$Y[k] = \sqrt{p_u}(\widehat{\mathbf{h}} * \mathbf{g})[L-1]X[k - \frac{L-1}{D}] + \sqrt{p_u} \sum_{l=0, l\neq(L-1)/D}^{(2L-2)/D} (\widehat{\mathbf{h}} * \mathbf{g})[Dl]X[k-l] + n[k] \quad (9)$$

where $n[k] \triangleq \widetilde{n}[Dk]$ and $p_u$ stands for the power amplifier.

Benefiting from temporal focusing, the power of $(\widehat{\mathbf{h}} * \mathbf{g})$ achieves its maximum at $(L-1)$ for $X[k - \frac{L-1}{D}]$, i.e.,

$$(\widehat{\mathbf{h}} * \mathbf{g})[L-1] = \frac{\sum_{l=0}^{L-1} \widehat{h}[l]\widehat{h}^*[l]}{\|\widehat{\mathbf{h}}\|} = \|\widehat{\mathbf{h}}\| \quad (10)$$

Consequently, the resulting signal-to-interference-plus-noise ratio (SINR) is obtained as

$$\text{SINR} = \frac{p_u \|\widehat{\mathbf{h}}\|^2}{p_u \sum_{l=0, l\neq(L-1)/D}^{(2L-2)/D} |(\widehat{\mathbf{h}} * \mathbf{g})[Dl]|^2 + \sigma_N^2} \quad (11)$$

assuming that each information symbol $X[k]$ has unit power.

Regarding the uplink, the previously designed signature waveform $\mathbf{g}$ serves as the equalizer at the AP side as shown in Fig. 2(c). Similar to the signal flow in the downlink scheme, the AP can detect the information symbol based on the temporal focusing of $(\widehat{\mathbf{h}} * \mathbf{g})$ in the uplink. Such a scheme of both downlink and uplink is defined as the asymmetric architecture, which provides the asymmetric complexity distribution between the AP and TD. In other words, the design philosophy of uplink is to keep the complexity of terminal users at minimal level.

Note that the homogeneous TR system can be easily extended to multi-user scenario according to the previous work [13], which exploits the spatial degrees of freedom in the environment and uses the multipath profile associated with each user's location as a location-specific signature for the user. In addition, different users are allowed to adopt different rate backoff factors to accommodate the heterogeneous QoS requirements for various applications in the IoT.

**Remark:** Even though the homogeneous TR system can support different QoS through varying $D$, all devices in the system must share the same bandwidth thus the sample rate, which increases the not only hardware cost but also computation burden for those low-end TDs. Besides the heterogenous QoS required by very diverse applications, the definition of heterogeneity in IoT should also cover the heterogeneous hardware capabilities (such as bandwidth, sample rate, computational and storage power and etc.), which apparently is not supported by the homogeneous TR system. Such more general heterogeneity requirement in the IoT motivates the heterogenous TR paradigm in this paper.

## III. Heterogenous Time-Reversal System

Even though the homogeneous TR system cannot handle bandwidth heterogeneity, the majority of challenges in the IoT can be tackled simultaneously through the TR technique [14]. Does there exist an efficient way to modify the existing homogenous TR system to handle the bandwidth heterogeneity while maintaining the most benefit of the TR technique? The answer is yes and the heterogeneous TR system is potentially the best candidate to address the issue.

Fig. 3: Spectrum Occupation of Heterogeneous TDs

In contrast with the same spectrum occupation of all devices in the homogenous setting, $N$ types of TDs with distinct spectrum allocation and bandwidths are supported simultaneously by a single AP in the heterogenous TR system. In other words, different types of TDs have the distinct carrier frequency ($f_{c_i}$) and bandwidth ($B_i$) as shown in Fig. 3.

### A. Modifications on homogenous TR system

In order to support the heterogenous TDs, several modifications need to be conducted at both AP and TD sides of the existing homogeneous TR system.

*1) TD side:* As stated before, heterogeneous TDs of different types have distinct $f_{c_i}$'s and $B_i$'s. First of all, the radio-frequency (RF) components of different types have to be distinct. Specifically, the oscillation frequency of the voltage-controlled oscillator (VCO) at type $i$ TD is set to $f_{c_i}$ and the bandwidth of analog bandpass filter is $B_i$. Then, the ADC deployed for type $i$ TDs has the sample rate of $f_{s_i} = \alpha B_i$ based on the previous discussion. Furthermore, various root-raised-cosine filters for different types are required, i.e., $\mathbf{RRC}_{B_i, f_{s_i}}$.

*2) AP side:* In order to support heterogeneous TDs simultaneously, the bandwidth of AP, denoted as $B_{AP}$, is the aggregated version of the bandwidth of all heterogeneous TDs. Even though more complicated digital signal processing is enforced to handle different data streams for various types, only one set of RF components is needed at the AP side. The digital signal processing includes frequency shift, rate convertor and root-raised-cosine filter. More specifically, a frequency shift component $\exp^{j\omega_i n}$ is implemented for each type to support multiple carrier frequencies. A distinct sample rate convertor (expander or decimator) with rate $\alpha B_{AP}/B_i$ is deployed for each type $i$ to enable the multirate processing. The root-raised-cosine filter $\mathbf{RRC}_{B_i, \alpha B_{AP}}$ for type $i$ is utilized to limit the effective bandwidth of signals for the heterogeneous TDs.

In the following, the detailed system mechanism together with the modified system architecture is developed for the proposed heterogeneous TR system.

### B. Channel probing phase

The channel probing phase of a type $i$ TD is shown in Fig. 4. Compared with the one in Fig. 2a, there exists some differences mentioned in the last subsection. Prior to the data transmission phase, an impulse is upsampled by $\alpha$, filtered by $\mathbf{RRC}_{B_i, \alpha B_i}[n]$ and transmitted out after going through the RF components at the TD side. The transmitted signal propagates to AP through the multipath channel $h_i(t)$, where

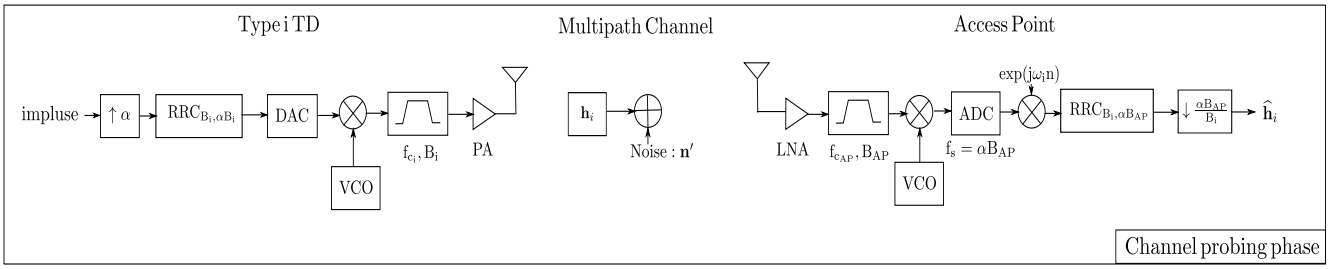


Fig. 4: Channel Probing of Type $i$ TD in Heterogeneous TR System

AP samples the received signal with a higher sample rate $f_s = \alpha B_{AP}$, shifts the signal to baseband (based on the difference between $f_{c_i}$ and $f_{c_{AP}}$), filters it through the other matched $\mathbf{RRC}_{B_i,\alpha B_{AP}}[n]$, downsamples the waveform by $\alpha B_{AP}/B_i$, and finally records the downsampled waveform as $\widehat{\mathbf{h}}_i$.

With sample rate $f_s = \alpha B_{AP}$, the discrete CIR can be written as

$$\overline{h}_i[n] = h_i(nT_s) \tag{12}$$

where $T_s = 1/(\alpha B_{AP})$.

Since the digital-to-analog convertor (DAC) serves the interpolator, the transmitted signal of the TD shown in Fig. 4 is mathematically equivalent to that generated through the following process, i.e., upsampled by $\alpha B_{AP}/B_i$, filtered by $\mathbf{RRC}_{B_i,\alpha B_{AP}}[n]$ and converted to analog signal by the DAC. Therefore, similarly according to the polyphase identity, the equivalent CIR for the type $i$ TD with bandwidth $B_i$ can be expressed as

$$\widehat{\mathbf{h}}_i = \sqrt{\beta_i}\big(\mathbf{RRC}_{B_i,\alpha B_{AP}} * \overline{\mathbf{h}}_i * \mathbf{RRC}_{B_i,\alpha B_{AP}}\big)_{[\alpha\beta_i]} \tag{13}$$

where $\beta_i = B_{AP}/B_i$ and $\sqrt{\beta_i}$ is used to compensate the power difference between $\mathbf{RRC}_{B_i,\alpha B_i}[n]$ and $\mathbf{RRC}_{B_i,\alpha B_{AP}}[n]$.

Even though the channel probing of a single type is evaluated here, it can be extended straightforward to multi-type TDs by deploying different digital processing for multi-type in parallel, e.g., frequency shift, RRC filtering and downsampling with type-specific factor. In other words, the AP can support heterogeneous TDs with one single set of RF components but more complicated digital processing.

### C. Data transmission phase

Suppose $N$ types of TDs are communicating with the AP simultaneously, where the number of TDs in type $i$ is denoted as $M_i$. Upon acquiring the equivalent CIRs, the signature waveform $\mathbf{g}_{i,j}$ is designed for $j^{th}$ TD in the type $i$ with various existing design methods. Take the basic TR signature design for example, i.e.,

$$g_{i,j}[n] = \frac{\widehat{h}^*_{i,j}[L-1-n]}{\|\widehat{\mathbf{h}}_{i,j}\|} \tag{14}$$

where $\widehat{\mathbf{h}}_{i,j}$ is defined in (13).

First, the downlink data transmission is considered. As shown in Fig. 5(a), let $\{X_{i,j}[k]\}$ be the the sequence of information symbols transmitted to the $j^{th}$ TD in type $i$. Similar to the case in the homogeneous TR system, a rate backoff factor $D_{i,j}$ is introduced to adjust the symbol rate, i.e., the symbol rate for $j^{th}$ TD in the type $i$ is $(B_i/D_{i,j})$. Then, the signature $\mathbf{g}_{i,j}$ is embedded into the TD-specific data stream $\mathbf{X}_{i,j}^{[D_{i,j}]}$ and the signature embedded symbols of the same type $i$ are merged together as $\mathbf{S}_i$, e.g.,

$$\mathbf{S}_i = \sum_{j=1}^{M_i} \left(\mathbf{X}_{i,j}^{[D_{i,j}]} * \mathbf{g}_{i,j}\right) \tag{15}$$

Later, the merged symbols $\mathbf{S}_i$ go through the type-specific digital signal processing, i.e., upsampled with factor $\alpha B_{AP}/B_i$, filtered by $\mathbf{RRC}_{B_i,\alpha B_{AP}}$ and carried to the type-specific digital frequency with frequency shift $\exp(-j\omega_i n)$. In the end, the processed data streams of $N$ types are mixed together and broadcasted to all the heterogeneous TDs through one set of RF components at the AP.

Regarding the receiver side, the $j^{th}$ TD in type $i$ is taken as an example. The broadcast signal propagates to the TD through the multipath profile $h_{i,j}(t)$. Later, the signal passes through the analog bandpass filter centering at $f_{c_i}$ with bandwidth $B_i$. Note that the filtered signal includes not only the intended signal but the interference, e.g., the inter-user-inference (IUI) from the TDs within the same type and the inter-type-interference (ITI) from the other types (whose spectrum overlaps with type $i$). Thanks to the spatio-temporal focusing effect, the interference is suppressed due to the unique multipath profile. Afterwards, the signal is carried to baseband and sampled with a sample rate $f_{s_i} = \alpha B_i$, which is much smaller than that at the AP for the low-end TDs. In the end, the sampled signal goes through $\mathbf{RRC}_{B_i,\alpha B_i}$ and the rate matching decimator to generate symbols $\{Y_{i,j}[k]\}$, based on which $\{X_{i,j}[k]\}$ are detected. The theoretical analysis regarding the signal-to-interference-plus-noise ratio (SINR) will be derived in the next section.

The system architecture of uplink is shown in Fig. 5(b). From the figure, the property of asymmetric architecture is preserved in the heterogeneous TR system. Same to the homogeneous TR system, the precoding signatures $\mathbf{g}_{i,j}$'s in the downlink serve as the equalizers in the uplink. After converting the signal into digital domain through a single set of RF components at the AP, multiple parallel digital processing (e.g., frequency shift, RRC filtering and rate conversion) is required to support $N$ types of TDs simultaneously.

**Remark:** Compared with the existing homogeneous TR system, the heterogenous TR system maintains the capability to support different QoS through not only varying the backoff

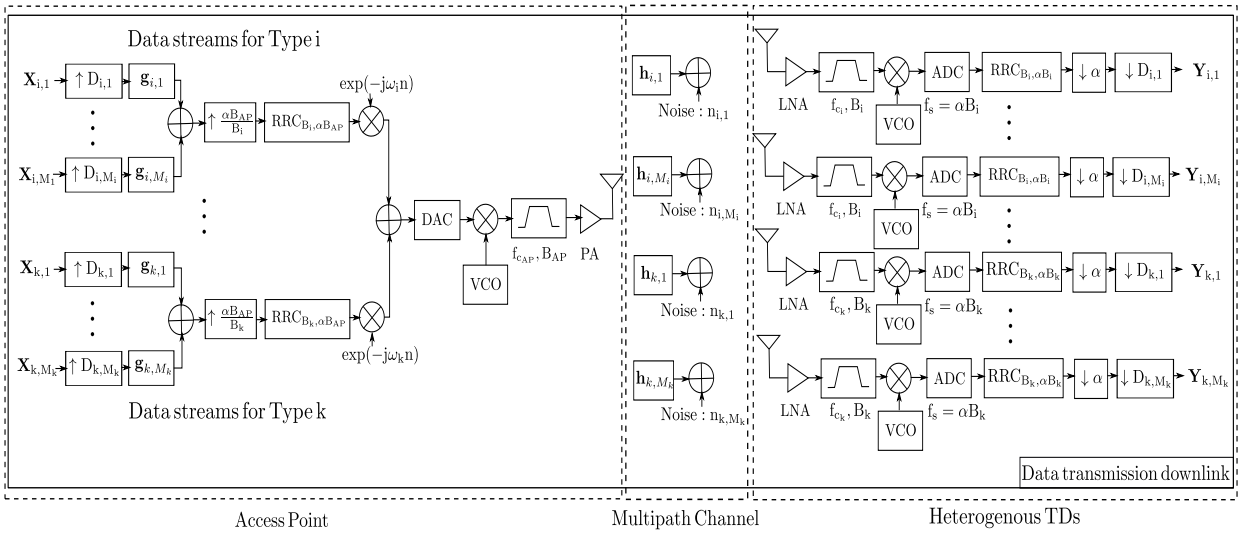


(a) Downlink

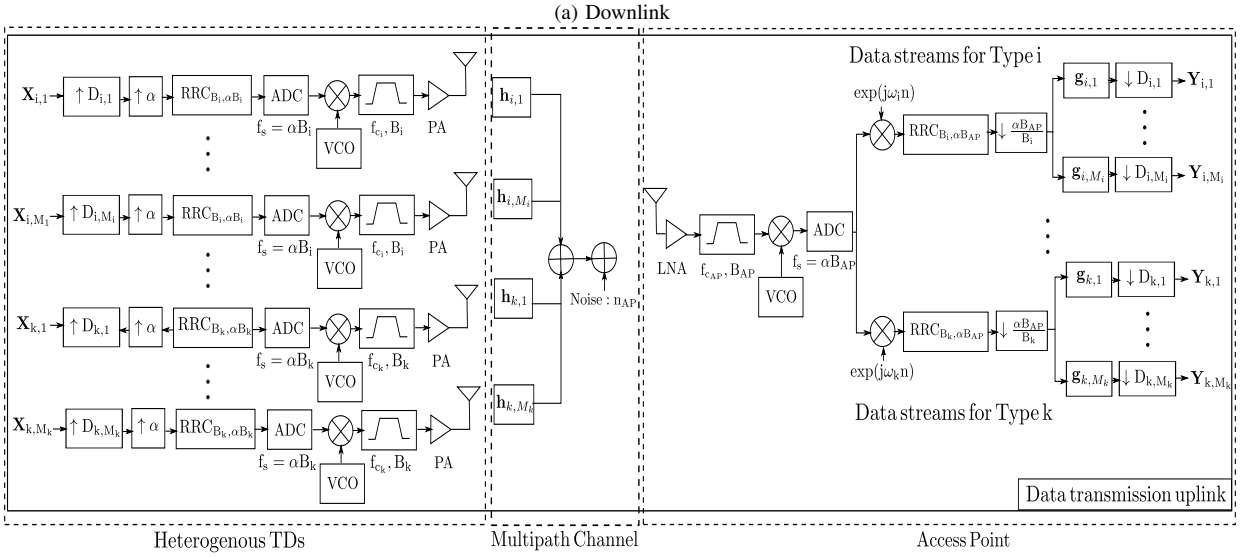


(b) Uplink

Fig. 5: Data Transmission in Heterogeneous TR System

factor $D_{i,j}$ but providing the flexibility for TDs to select various $B_i$'s. More importantly, the heterogeneous TR system architecture further promotes the benefit of the asymmetric complexity. In other words, the new modifications enhance the concentration of the complexity at the AP side. Regarding the AP, a single set of RF components is required. Even though more complicated parallel digital signal processing is needed, it can be easily satisfied with more powerful DSP unit at an affordable cost and complexity. Regarding the heterogeneous TDs, the ADC sample rate is reduced significantly for those devices with smaller bandwidth, which lowers down the cost of hardware dramatically for the low-end TDs. In addition, the lower sample rate naturally decreases the computational burden as well.

## IV. Performance Analysis of Heterogeneous TR System

In this section, we conduct some theoretic analysis on the proposed heterogeneous TR system and evaluate the SINR for the individual TD. Without loss of generality, the downlink scenario is investigated here. Due to the asymmetric architecture and channel reciprocity, the uplink scenario can be analyzed similarly. In the following, two special cases in the heterogeneous TR system are first studied. Then, the analysis of a specific TD in the general setting is derived through extending the results of the special cases.

### A. Overlapping Case

First, a special case of heterogenous TR system is considered. Suppose there are only two types of TDs in the system, e.g., type $i$ and type $k$. As shown in Fig. 6, both types share the same carrier frequency with AP, whose spectrum is overlapped. Without loss of generality, only a single TD is assumed to exist within each type.

In this special case, the downlink system architecture in Fig. 5(a) can be significantly simplified. In the first place, the frequency shift can be removed due to the same carrier

Fig. 6: Spectrum Occupation of Case I

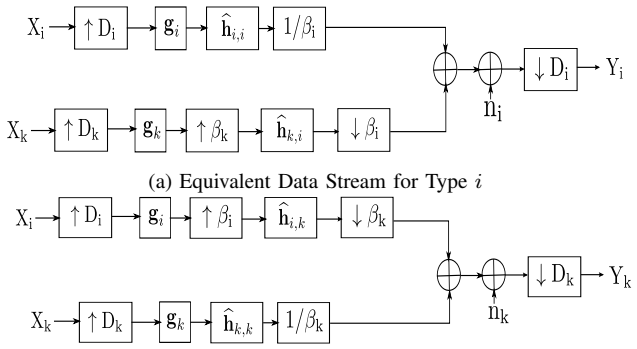

(a) Equivalent Data Stream for Type $i$

(b) Equivalent Data Stream for Type $k$

Fig. 7: Equivalent Architecture in Case I

frequency. Moreover, the analog bandpass filter could also be ignored in the analysis since the effective bandwidth has already been limited by the RRC filters. Denote $\widehat{\mathbf{h}}_{a,b}$ as the equivalent CIR for the type $a$ symbols sent from the AP to the type $b$ TD. Based on (4), we have

$$\widehat{\mathbf{h}}_{a,a} = \sqrt{\beta_a}\left(\mathbf{RRC}_{B_a,\alpha B_{AP}} * \overline{\mathbf{h}}_a * \mathbf{RRC}_{B_a,\alpha B_{AP}}\right)_{[\alpha\beta_a]} \tag{16}$$

In addition, the equivalent CIR for interference can be derived as follows through utilizing the noble identities [17],

$$\widehat{\mathbf{h}}_{a,b} = \left(\mathbf{RRC}_{B_a,\alpha B_{AP}} * \overline{\mathbf{h}}_b * \mathbf{RRC}^{[\beta_b]}_{B_b,\alpha B_b}\right)_{[\alpha]} \tag{17}$$

where $a, b \in \{i, k\}$, $\beta_a = B_{AP}/B_a$ and $\overline{\mathbf{h}}_a$ is the discrete CIR from the AP to the type $a$ TD with sample rate $f_s = \alpha B_{AP}$.

Upon acquiring the equivalent CIRs, the signature for each type is designed, e.g.,

$$g_a[n] = \frac{\widehat{h}^*_{a,a}[L-1-n]}{\|\widehat{\mathbf{h}}_{a,a}\|} \tag{18}$$

where $a \in \{i, k\}$. Note that there exists focusing effect of the term $(\mathbf{g}_a * \widehat{\mathbf{h}}_{a,a})$ based on (18). Therefore, the simplified system model is shown in Fig. 7 base on the equations above.

From the figure, the received symbols at type $i$ TD can be expressed as

$$\begin{aligned} Y_i[n] = &\frac{\sqrt{p_u}}{\beta_i}\left(\mathbf{g}_i * \widehat{\mathbf{h}}_{i,i}\right)[L_i - 1]X_i[n - \frac{L_i - 1}{D_i}] \\ &+ \frac{\sqrt{p_u}}{\beta_i}\sum_{l=0,l\neq(L_i-1)/D_i}^{(2L_i-2)/D_i}\left(\mathbf{g}_i * \widehat{\mathbf{h}}_{i,i}\right)[D_i l]X_i[n-l] \\ &+ \sqrt{p_u}\sum_{l=0}^{(L_{k,i}-1)/(\beta_k D_k)}\left(\mathbf{g}_k^{[\beta_k]} * \widehat{\mathbf{h}}_{k,i}\right)[\beta_k D_k l]\, X_k[n-l] \\ &+ n_i[n] \end{aligned} \tag{19}$$

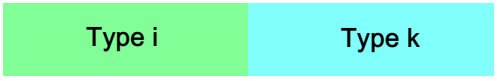


Fig. 8: Spectrum Occupation of Case II

where $p_u$ is the power amplifier, $L_i = \text{length}\left(\widehat{\mathbf{h}}_{i,i}\right)$ and $L_{k,i} = \text{length}\left(\mathbf{g}_k^{[\beta_k]} * \widehat{\mathbf{h}}_{k,i}\right)$.

In (19), the first and second term are the typical expected signal term and ISI term, respectively. In addition, the third term is the inter-type-interference (ITI) from the type $k$ TD. Moreover, based on the spatio-temporal focusing effect in the TR system, the ITI is suppressed naturally with the location-specific signature. A similar equation of the received symbols can be derived for the type $k$ TD.

Since the frequency shift $\exp^{-j\omega_i n}$ has unitary power, the analysis in (20) is also applied for the case where the carrier frequency of type $i$ and $k$ are different as long as their spectrum is overlapped.

### B. Non-overlapping Case

Another special case, where the spectrum of different types is non-overlapped, is considered in this subsection. Suppose two types of TDs exist in the system, e.g., type $i$ and type $k$, each of which contains a single TD. As shown in Fig. 8, there are no ITI between non-overlapped types due to the corresponding analog bandpass filters and RRC filters. Therefore, the analysis becomes straightforward and the received symbols at type $i$ TD is derived as,

$$\begin{aligned} Y_i[n] = &\frac{\sqrt{p_u}}{\beta_i}\left(\mathbf{g}_i * \widehat{\mathbf{h}}_{i,i}\right)[L_i - 1]X_i[n - \frac{L_i - 1}{D_i}] \\ &+ \frac{\sqrt{p_u}}{\beta_i}\sum_{l=0,l\neq(L_i-1)/D_i}^{(2L_i-2)/D_i}\left(\mathbf{g}_i * \widehat{\mathbf{h}}_{i,i}\right)[D_i l]X_i[n-l] \\ &+ n_i[n] \end{aligned} \tag{20}$$

which is well studied in the homogeneous TR system [12].

### C. Mixed Case

Based on the previous analysis of two special cases, the heterogeneous TR system is analyzed under the general scenario, where $N$ types of TDs are supported in the system and the number of type $i$ TD is $M_i$. The spectrum of different types is shown in Fig. 3.

As discussed in Section III, $\{X_{i,j}[k]\}$ denotes the information symbols for the $j^{th}$ TD in type i, and $D_{i,j}$ and $\mathbf{g}_{i,j}$ are the backoff factor and the embedded signature for the symbols $\{X_{i,j}[k]\}$, respectively. Based on Section IV-A, the TDs in type $i$ suffer ITI from type $k$ TDs, where $k \in T_i$ and $T_i$ denotes the set of types whose spectrum is overlapped with type $i$. In other words, the data streams of type $k$, where $k \notin T_i$, causes no interference to type $i$ TDs according to Section IV-B.

Regarding the CIR, denote $\overline{\mathbf{h}}_{i,j}$ as the discrete CIR from the AP to the $j^{th}$ TD in type $i$ with sample rate $f_s = \alpha B_{AP}$. Moreover, let $\widehat{\mathbf{h}}_{i_m,k_n}$ be the equivalent CIR for the data stream

of $m^{th}$ TD in type $i$ between the AP to $n^{th}$ TD in type $k$. Similar to (16) and (17), the equivalent CIR for data streams can be derived as

$$\widehat{\mathbf{h}}_{i_m,k_n} = \begin{cases} \sqrt{\beta_i}\left(\mathbf{RRC}_{B_i,\alpha B_{AP}} * \overline{\mathbf{h}}_{i,n} * \mathbf{RRC}_{B_i,\alpha B_{AP}}\right)_{[\alpha\beta_i]} & i = k \\ \left(\mathbf{RRC}_{B_i,\alpha B_{AP}} * \overline{\mathbf{h}}_{k,n} * \mathbf{RRC}^{[\beta_k]}_{B_k,\alpha B_k}\right)_{[\alpha]} & i \neq k \end{cases} \tag{21}$$

where $\beta_i = B_{AP}/B_i$. From (21), the length of the equivalent CIR solely depends on the types of data stream and the receiving TD. Once the CIRs are estimated, various signature design methods can be deployed. Take the basic TR signature of the $j^{th}$ TD of type $i$ for example, i.e.,

$$g_{i,j}[n] = \frac{\widehat{h}^*_{i_j,i_j}[L-1-n]}{\|\widehat{\mathbf{h}}_{i_j,i_j}\|} \tag{22}$$

Thus the received symbols at the $j^{th}$ of type $i$ TD $\mathbf{Y}_{i,j}$ can be expressed as

$$\begin{aligned} & Y_{i,j}[n] \\ &= \frac{\sqrt{p_u}}{\beta_i}\left(\mathbf{g}_{i,j} * \widehat{\mathbf{h}}_{i_j,i_j}\right)[L_i-1]X_{i,j}[n-\frac{L_i-1}{D_{i,j}}] \\ &+ \frac{\sqrt{p_u}}{\beta_i}\sum_{l=0,l\neq(L_i-1)/D_{i,j}}^{(2L_i-2)/D_{i,j}}\left(\mathbf{g}_{i,j} * \widehat{\mathbf{h}}_{i_j,i_j}\right)[D_{i,j}l]X_{i,j}[n-l] \\ &+ \frac{\sqrt{p_u}}{\beta_i}\sum_{\substack{m=1\\m\neq j}}^{M_i}\sum_{l\neq(L_i-1)/D_{i,m}}^{(2L_i-2)/D_{i,m}}\left(\mathbf{g}_{i,m} * \widehat{\mathbf{h}}_{i_m,i_j}\right)[D_{i,m}l]X_{i,m}[n-l] \\ &+ \sqrt{p_u}\sum_{k\in T_i}\sum_{m=1}^{M_k}\sum_{l=0}^{\frac{L_{k,i}-1}{\beta_k D_{k,m}}}\left(\mathbf{g}^{[\beta_k]}_{k,m} * \widehat{\mathbf{h}}_{k_m,i_j}\right)[\beta_k D_{k,m}l]\,X_{k,m}[n-l] \\ &+ n_{i,j}[n] \end{aligned} \tag{23}$$

where $L_i = \text{length}\left(\widehat{\mathbf{h}}_{i_*,i_*}\right)$, $\beta_i = B_{AP}/B_i$ and $L_{k,i} = \text{length}\left(\mathbf{g}^{[\beta_k]}_{k,*} * \widehat{\mathbf{h}}_{k_*,i_*}\right)$.

In (23), the first term is the intended signal, the second and third term represents the ISI and the IUI within the same type and the ITI from overlapped types ($k \in T_i$) is expressed as the fourth term. Based on (23), the SINR for the $j^{th}$ TD in type i within the general heterogeneous TR system can be calculated correspondingly like (11).

## V. Simulation Results

In this section, we conduct simulations to evaluate the BER performance of the heterogeneous TR system under various settings. We assume that $N$ types of TDs coexist in the system with single or multiple devices within each type. Different types devices have heterogenous bandwidths, spectrum occupation, hardware capabilities and QoS requirement. The CIR used in the simulation is based on the ultra-wide band (UWB) channel model [21].

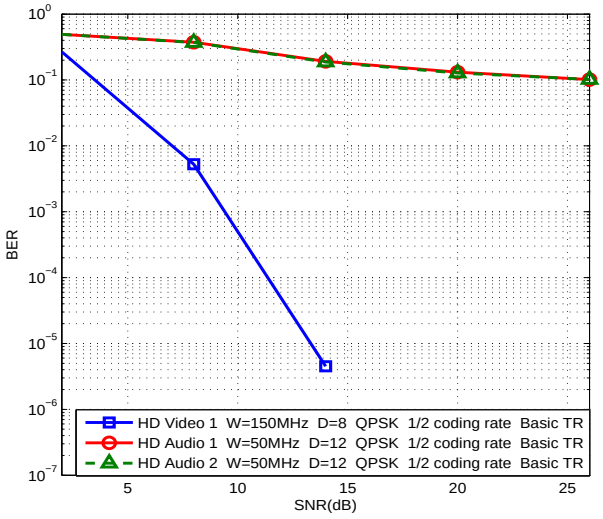


Fig. 9: BER performance of 3 devices where 2 HD audio devices are included in the same type with basic TR signature.

### A. TDMA and Spectrum Allocation

We first consider 3 devices in the heterogeneous TR system, whose features are listed in Table I. According to the table, the bit rates of the HD video and the HD audio are around 18 Mbits/s and 4 Mbits/s. Based on previous discussion, the bandwidth of AP is assumed to be 150MHz to support simultaneous data transmission to these 3 devices.

We first consider the case that 3 devices are categorized into 2 types, where Type 1 includes the HD video device and Type 2 consists 2 HD audio devices. The BER performance of 3 devices under such scenario is shown in Fig. 9. Inferred from the figure, the BER performance of the 2 HD audio devices is much worse compared with the BER of HD video. The reason behind is that the suppression of IUI in the TR system heavily depends on the number of resolved independent multipaths, which increases with the bandwidth. Since the bandwidth of two HD audio is much narrower, the IUI from the other devices becomes severer with the basic TR signature. In order to tackle the IUI for the devices with a narrower bandwidth, along with the TR technology, other techniques have to be considered in the heterogenous TR system as well.

We first consider applying time division multiple access (TDMA) to the heterogeneous TR system. In other words, the AP supports one HD audio at a time. To maintain the same QoS requirement in terms of bit rate, either adjusting the coding rate or decreasing the backoff factor is adopted in the system. The improved BER performance of 3 devices with simple waveform design is shown in Fig. 10, where (a) removes the channel coding and (b) decreases the backoff rate to maintain the same bit rate for the HD audio. Compared with the BER in Fig. 9, the BER performance is improved significantly with the simple waveform design. Moreover, decreasing backoff factor to maintain the bit rate seems to be a better strategy for the devices with narrow bandwidth through comparing (a) and (b). Note that there are some waveform

| Device Name | Bandwidth (MHz) | Backoff Factor | Modulation | Coding Rate | Waveform Design |
|---|---|---|---|---|---|
| HD Video 1 | 150 | 8 | QPSK | 1/2 | Basic TR |
| HD Audio 1 | 50 | 12 | QPSK | 1/2 | Basic TR |
| HD Audio 2 | 50 | 12 | QPSK | 1/2 | Basic TR |

TABLE I: Features of 1 HD Video and 2 HD Audio

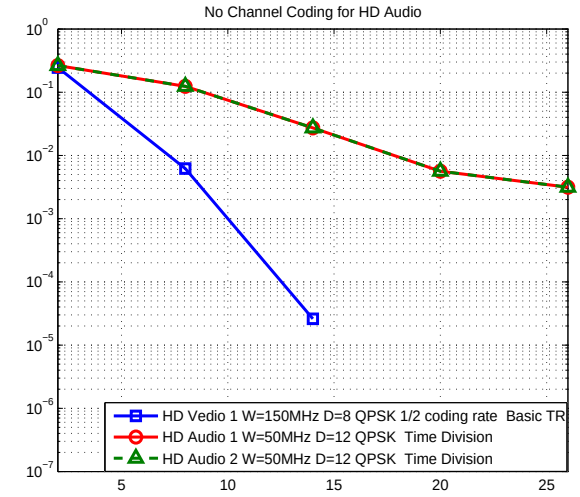


(a) No channel coding to maintain the same bit rate.

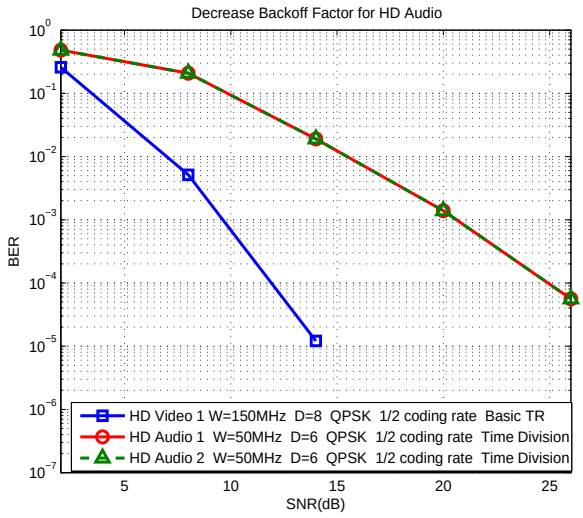


(b) Decrease backoff factor to maintain the same bit rate.

Fig. 10: Improved BER performance with TDMA for the HD audio

design techniques [19] that potentially can be implemented in the heterogeneous TR system with even better performance.

Even though a narrow bandwidth decreases the number of resolved independent multipaths thus resulting in severer IUI, a narrow bandwidth on the other hand provides more flexibility for spectrum allocation. Therefore, another way to improve the BER performance in Fig. 9 is to arrange the spectrum occupation smartly thus removing the unnecessary interference. For example, 3 devices in Table I can be categorized into 3

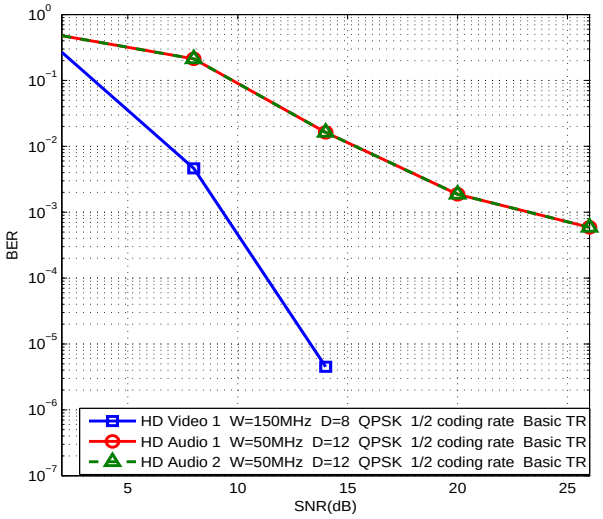


Fig. 11: Improved BER performance with spectrum allocation for the HD audio

distinct types, where two HD audio devices are allocated into 2 spectrally non-overlapped types. Then the improved BER performance with the spectrum allocation is shown in Fig. 11.

### *B. Heterogeneous TR System versus Homogeneous TR System*

As discussed in the previous subsection, appropriate spectrum allocation can significantly improve the BER performance even with a narrow bandwidth in the heterogeneous TR system. In other words, the narrow bandwidth under heterogeneous setting does not necessarily lead to worse BER performance compared with the wide bandwidth under homogeneous setting. Inspired by that, we investigate the BER performance of the devices in both homogeneous and heterogeneous TR system under the same bit rate.

Assume there exists three devices with bit rate requirement of 12.5 Mbits/s supported by a TR AP with 150 MHz bandwidth. Suppose the devices have flexible hardware capabilities, i.e., the carrier frequency and the bandwidth. To support these devices, two potential paradigms, homogeneous paradigm and heterogeneous paradigm, are available. For the sake of fairness, the basic TR signature is adopted in both paradigms.

In the homogeneous setting, all three devices occupy the 150 MHz spectrum with QPSK modulation and backoff factor $D = 12$. A channel coding with 1/2 coding rate is employed. In the heterogeneous setting, the devices are categorized into three non-overlapped types. More specifically, three devices with 50MHz bandwidth are allocated into three non-overlapped

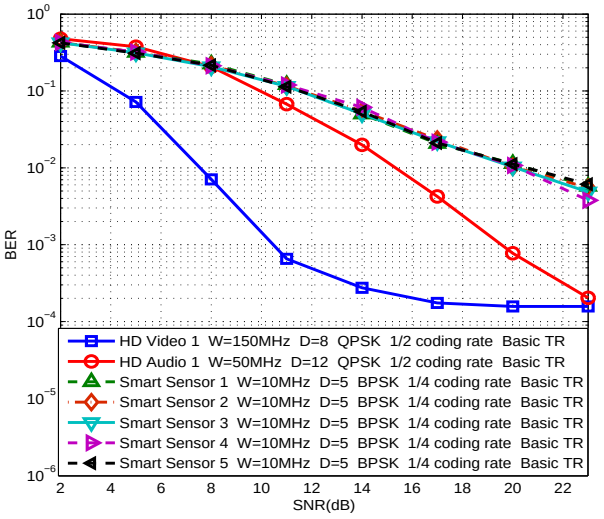


Fig. 12: BER Performance of the Devices in Smart Homes

spectrum. To maintain the same bit rate, a backoff factor $D = 4$ is implemented. Their BER performance is shown in Fig. 13. From the figure, the BER performance of the homogeneous paradigm saturates fast, which is due to the well-known fact that ISI and IUI would dominate the noise with the basic TR signature at high SNR region [19]. However, the IUI is better tackled in the heterogenous paradigm with smart spectrum allocation even though the number of independent multipaths resolved by the narrower bandwidth becomes fewer. Therefore, the performance of the heterogeneous paradigm can be even better than that of the homogeneous paradigm with additional techniques like spectrum allocation.

### C. Heterogeneous TR System Case Study: Smart Homes

In this subsection, we choose Smart Homes as an example of the IoT application to test the BER performance with the heterogeneous TR paradigm. Instrumenting buildings with the IoT technologies will help in not only reducing resources (electricity, water) consumption but also in improving the satisfaction level of humans. Typically, the HD video and HD audio are employed in the Smart Homes for both the security monitoring and entertainment. Moreover, smart sensors are used in the Smart Homes to both monitor resource consumptions as well as to proactively detect the users' need. Therefore, in the following simulation, we assume 1 HD video, 1 HD audio and 5 smart sensors in the Smart Homes are supported by the heterogeneous TR paradigm. The specific features of these devices are listed in Table II and the corresponding BER performance is shown in Fig 12. Note the saturation of the BER for the HD video is due to the dominant IUI with the basic TR signature. In addition, the slight difference in the BER for the smart sensors comes from the frequency-selectivity of the channel.

## VI. Conclusion

A novel TR-based heterogeneous communication system is developed to support devices with various bandwidths

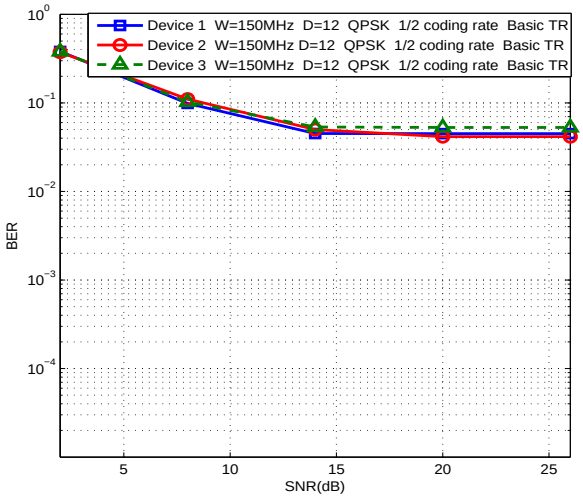


(a) Homogeneous Paradigm

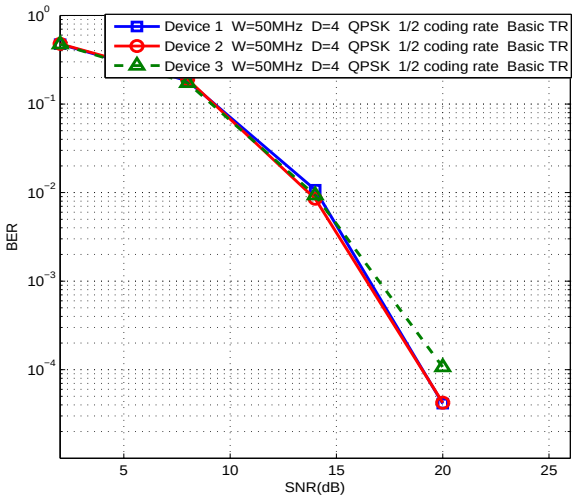


(b) Heterogeneous Paradigm

Fig. 13: BER Comparison of Homogeneous Paradigm and Heterogeneous Paradigm with Basic TR Signature

in IoT. Different from building middlewares, the proposed approach enables connectivity between devices with heterogeneous bandwidth requirement by means of multirate signal processing. In this way, the complexity of the proposed system mostly lies in the parallel digital processing at the AP side, which can be easily handled with more powerful DSP, while maintaining low complexity of the TDs. System performance is evaluated through both theoretical analysis and simulations, which show a significant BER improvement with appropriate spectrum allocation.

## References

[1] J. Gubbi, R. Buyya, S. Marusic, and M. Palaniswami, "Internet of things (iot): A vision, architectural elements, and future directions," *Future Generation Computer Systems*, vol. 29, no. 7, pp. 1645–1660, 2013.

[2] K. Ashton, "That internet of things thing," *RFiD Journal*, vol. 22, no. 7, pp. 97–114, 2009.

| Device Name | Bandwidth (MHz) | Backoff Factor | Modulation | Coding Rate | Waveform Design |
|---|---|---|---|---|---|
| HD Video 1 | 150 | 8 | QPSK | 1/2 | Basic TR |
| HD Audio 1 | 50 | 12 | QPSK | 1/2 | Basic TR |
| Smart Sensor 1 | 10 | 10 | QPSK | 1/2 | Basic TR |
| Smart Sensor 2 | 10 | 10 | QPSK | 1/2 | Basic TR |
| Smart Sensor 3 | 10 | 10 | QPSK | 1/2 | Basic TR |
| Smart Sensor 4 | 10 | 10 | QPSK | 1/2 | Basic TR |
| Smart Sensor 5 | 10 | 10 | QPSK | 1/2 | Basic TR |

TABLE II: Features of Devices in the Smart Homes


[3] H. Sundmaeker, P. Guillemin, P. Friess, and S. Woelfflé, "Vision and challenges for realising the internet of things," 2010.

[4] J. Buckley, *The Internet of Things: From RFID to the Next-Generation Pervasive Networked Systems*. Auerbach Publications, Nework York, 2006.

[5] L. Atzori, A. Iera, and G. Morabito, "The internet of things: A survey," *Computer networks*, vol. 54, no. 15, pp. 2787–2805, 2010.

[6] National Intelligence Coucil, "Disruptive civil technologies - six technologies with potential impacts on us interests out to 2025 - conference report cr 2008-07," http://www.dni.gov/nic/NIC_home.html, 2008.

[7] E. De Poorter, I. Moerman, and P. Demeester, "Enabling direct connectivity between heterogeneous objects in the internet of things through a network-service-oriented architecture," *EURASIP Journal on Wireless Communications and Networking*, vol. 2011, no. 1, pp. 1–14, 2011.

[8] M. Zorzi, A. Gluhak, S. Lange, and A. Bassi, "From today's intranet of things to a future internet of things: a wireless-and mobility-related view," *Wireless Communications, IEEE*, vol. 17, no. 6, pp. 44–51, 2010.

[9] S. de Deugd, R. Carroll, K. Kelly, B. Millett, and J. Ricker, "Soda: Service oriented device architecture," *Pervasive Computing, IEEE*, vol. 5, no. 3, pp. 94–96, July 2006.

[10] P. Spiess, S. Karnouskos, D. Guinard, D. Savio, O. Baecker, L. Souza, and V. Trifa, "Soa-based integration of the internet of things in enterprise services," pp. 968–975, July 2009.

[11] J. Pasley, "How bpel and soa are changing web services development," *Internet Computing, IEEE*, vol. 9, no. 3, pp. 60–67, May 2005.

[12] B. Wang, Y. Wu, F. Han, Y.-H. Yang, and K. J. R. Liu, "Green wireless communications: a time-reversal paradigm," *IEEE Journal on Selected Areas in Communications*, vol. 29, no. 8, pp. 1698–1710, 2011.

[13] F. Han, Y.-H. Yang, B. Wang, Y. Wu, and K. J. R. Liu, "Time-reversal division multiple access over multi-path channels," *IEEE Transactions on Communications*, vol. 60, no. 7, pp. 1953–1965, 2012.

[14] Y. Chen, F. Han, Y.-H. Yang, H. Ma, Y. Han, C. Jiang, H.-Q. Lai, D. Claffey, Z. Safar, and K. J. R. Liu, "Time-reversal wireless paradigm for green internet of things: An overview," *IEEE Internet of Things Journal*, vol. 1, no. 1, pp. 81–98, Feb 2014.

[15] I. Glover and P. M. Grant, *Digital communications*. Pearson Education, 2010.

[16] A. V. Oppenheim, R. W. Schafer, J. R. Buck *et al.*, *Discrete-time signal processing*. Prentice-hall Englewood Cliffs, 1989.

[17] P. P. Vaidyanathan, *Multirate systems and filter banks*. Pearson Education India, 1993.

[18] R. Daniels and R. Heath, "Improving on time reversal with miso precoding," *Proceedings of the Eighth International Symposium on Wireless Personal Communications Conference*, pp. 18–22, 2005.

[19] Y.-H. Yang, B. Wang, W. S. Lin, and K. J. R. Liu, "Near-optimal waveform design for sum rate optimization in time-reversal multiuser downlink systems," *IEEE Transactions on Wireless Communications*, vol. 12, no. 1, pp. 346–357, 2013.

[20] M. Emami, M. Vu, J. Hansen, A. Paulraj, and G. Papanicolaou, "Matched filtering with rate back-off for low complexity communications in very large delay spread channels," *Conference Record of the Thirty-Eighth Asilomar Conference on Signals, Systems and Computers*, vol. 1, pp. 218–222, Nov 2004.

[21] J. Foerster, "Channel modeling sub-committee report final," *IEEE P802. 15-02/368r5-SG3a*, 2002.